



SIX- ROTOR UAV HELICOPTER DYNAMICS AND CONTROL: THEORY AND SIMULATION

Abhishek¹, Abhinandan Tripathi²

Graduate Student, Electronics and Communication Engineering, Hanyang University, South Korea¹

Undergraduate Student, Mechanical Engineering, Indian Institute of Technology Guwahati, India²

ABSTRACT: The dynamical model of an original six-rotor is presented in this paper. The helicopter is composed of six rotors with constant pitch propellers; the six rotors are arranged as three counter-rotating offset pairs mounted at vertices of a triangular frame, with matched sets of counter-rotating rotor blades. Differential thrust from these three equally spaced points make helicopter able to manoeuvre quickly and precisely. Euler–Lagrange approach is used to obtain the dynamical model. Classical Linear Feedback control and nonlinear control strategy are proposed for control. The roll and the forward displacement are controlled by using a nested saturation control law. The pitch and lateral displacement are controlled in a similar way.

Keywords: Helicopter, Mini-rotorcraft, Non-linear control, 3 Point six rotors (3P-MAV6).

I. INTRODUCTION

Autonomous mini-aerial vehicles are proving their utility in numerous civil and military applications. The improvement of the capabilities of the existing flying vehicles requires contributions from different disciplines including aeronautics, electronics, signal processing, computer science etc. Similar to classical helicopter, a UAV should be able to perform hover as well as forward flight. A three-point six-rotor MAV (3P-MAV6) is an interesting alternative to the classical helicopter. A 3P-MAV6 is mechanically simpler than a helicopter since it has propellers with constant pitch and does not require a swash plate. The 3P-MAV6 maintenance is therefore simpler than that of a classical helicopter.

In view of the interest for the development of micro-UAV, several different aero dynamical configurations have been studied [1-4]. The paper focuses on a multi-rotor rotorcraft having six rotors with constant pitch propellers and no swash plate. The innovative design has three counter-rotating offset pairs mounted at the vertices of an equilateral triangle. It is clear that one of the advantages of 3P-MAV6 with respect to quad rotors and classical helicopter is that the offset layout doubles the thrust without increasing the size of the footprint, and naturally eliminates loss of efficiency due to torque compensation. Coaxial mounting of rotors ensures single point torque balancing. Moreover, if a motor malfunctions, the presence of its coaxial counter-pair mitigates risk and ensures safe landing.

The work presented in this paper focuses on the six-rotor MAV which was fabricated in manufacturing laboratory. The three upper rotors rotate in clockwise direction and the lower three in opposite direction. The angular velocity of the rotors can be adjusted to achieve desired roll, pitch and yaw.

II. CHARACTERISTICS OF THE 3P-MAV6

The following illustrations depict the control approach in broad sense. Fig. (1). The force \mathbf{f}_i produced by motor i is proportional to the square of the angular speed, that is $\mathbf{f}_i = k\boldsymbol{\omega}_i^2$, where k is coefficient of thrust of the propeller. Since each motor turns in a fixed direction, the produced force \mathbf{f}_i is always positive. The main thrust is sum of individual thrust of each motor i.e.

$$\mathbf{u} = \sum_{i=1}^6 \mathbf{f}_i = k \sum_{i=1}^6 \boldsymbol{\omega}_i^2 \quad (1)$$

The pitch and roll torque are functions of the difference in thrust and the Yaw torque is the sum $\tau_{M1} + \tau_{M2} + \tau_{M3} + \tau_{M4} + \tau_{M5} + \tau_{M6}$, where τ_{Mi} is the reaction torque of motor i due to shaft acceleration and the blade's drag. Using Newton's second law and neglecting shaft friction, we have $\mathbf{IM}_i \dot{\boldsymbol{\omega}}_i^2 = -\mathbf{b}\boldsymbol{\omega}_i^2 + \tau_{Mi}$, where \mathbf{IM} is the angular momentum of the i^{th}

International Journal of Advanced Research in Electrical, Electronics and Instrumentation Engineering

(An ISO 3297: 2007 Certified Organization)

Vol. 2, Issue 11, November 2013

motor and $b > 0$ is a constant. In steady state, that is, when $\dot{\omega}_i = 0$, the yaw torque is

$$\tau_{\psi} = b(\omega_1^2 + \omega_3^2 + \omega_5^2 - \omega_2^2 - \omega_4^2 - \omega_6^2) \quad (2)$$

The following motions can be accomplished keeping the total thrust, \mathbf{u} constant.

A. Roll motion:

Roll motion is attained using lateral motors. It can be done by increasing speed of (M1, M2) and decreasing speed of (M5, M6) simultaneously. Fig.(3)

B. Pitch motion:

Pitch motion is attained using differential thrust by front and rear motors. It is achieved by increasing speed of (M3, M4) and decreasing speed of (M1, M2) and (M5, M6) simultaneously. Fig. (2)

C. Yaw Motion:

Yaw motion is obtained by increasing the torque of the top motors, τ_{M1} , τ_{M3} and τ_{M5} , respectively, while decreasing the torque of the bottom motors, τ_{M2} , τ_{M4} and τ_{M6} . Fig. (4)

D. Forward Motion:

Forward motion is attained by pitching. This motion is obtained by increasing the speed of the rear motors (M3, M4) equally while reducing the speed of the front motors (M1, M2) and (M5, M6). Similarly, the backward motion can also be achieved. Fig. (2)

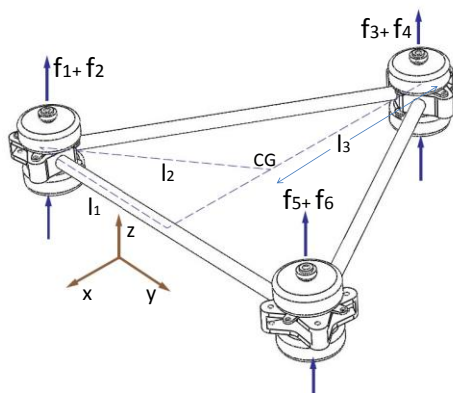


Fig. 1. CAD Model representing Thrust.

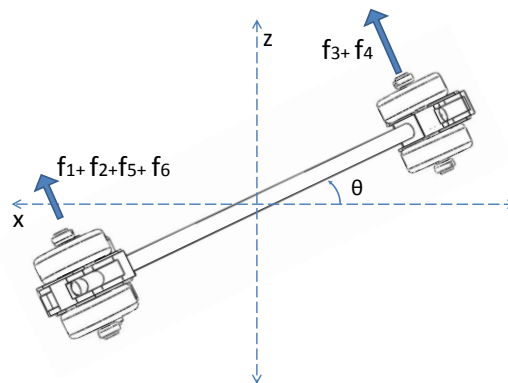


Fig. 2. Pitch and forward motion.

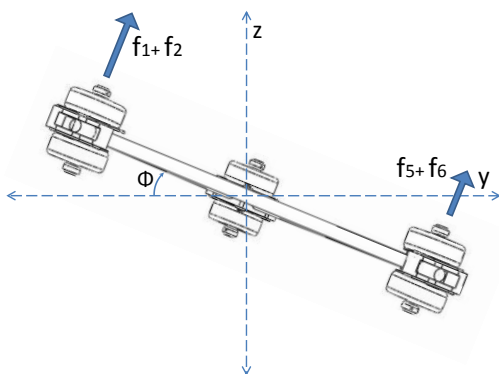


Fig. 3. Roll

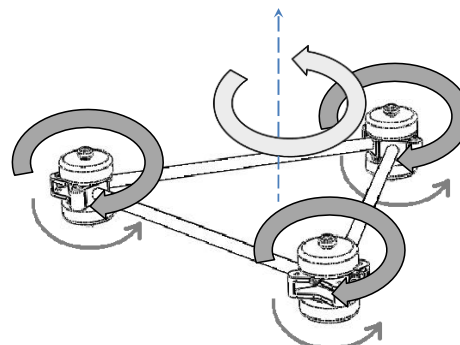


Fig. 4. Yaw.



International Journal of Advanced Research in Electrical, Electronics and Instrumentation Engineering

(An ISO 3297: 2007 Certified Organization)

Vol. 2, Issue 11, November 2013

III. DYNAMICAL MODEL

This section presents the dynamical model of the 3P-MAV6 using the Euler-Lagrange approach. The following is a derivation of the equations of motion for the rotor-craft assuming it is a rigid body evolving in a 3-D space acted on by gravity, thrust forces and reaction torques generated by the propellers. The dynamics of the six electric motors are fast and, thus, are neglected. Wind disturbances and change in propeller effective pitch with changes in free stream velocity as observed by the propeller (due to vehicle translation and rotation) are also neglected. The generalized coordinates describing rotorcraft position and orientation are

$$\mathbf{q}^T = (\mathbf{x}, \mathbf{y}, \mathbf{z}, \psi, \theta, \phi) \in R^6 \quad (3)$$

where $\xi = (x, y, z) \in R^3$ denotes the position of the center of mass of the rotorcraft relative to the fixed inertial frame I and $\eta = (\psi, \theta, \phi) \in R^3$ are the three Euler angles. Ψ is the yaw angle around the z-axis; θ is the pitch angle around the modified y-axis and ϕ is the roll angle around modified z-axis which represents the orientation of the rotorcraft. Model is now separated into rotational and translational coordinates, respectively.

$$\xi^T = (\mathbf{x}, \mathbf{y}, \mathbf{z}) \in R^3 \quad (4)$$

$$\eta^T = (\psi, \theta, \phi) \in R^3 \quad (5)$$

The translational kinetic energy of the rotorcraft is given by,

$$KE_{tra} = \frac{1}{2} m \xi^T \dot{\xi} \quad (6)$$

where, m denotes the mass of the rotorcraft. The rotational kinetic energy is $KE_{rot} = (1/2)\omega^T I \omega$ where ω is the angular velocity, I is the inertia matrix. The angular velocity vector ω resolved in the body fixed frame is related to the generalized velocities $\dot{\eta}$ (in the region where the Euler angles are valid) by means of the kinematic relationship

$$\dot{\eta} = W_b^{-1} \omega \quad (7)$$

$$W_b = \begin{bmatrix} -\sin \theta & 0 & 1 \\ \cos \theta \sin \psi & \cos \psi & 0 \\ \cos \theta \cos \psi & -\sin \psi & 0 \end{bmatrix} \quad (8)$$

Now, $J = J(\eta)$ is defined as

$$J = W_b^T I W_b \quad (9)$$

$$\therefore KE_{rot} = \frac{1}{2} \dot{\eta}^T J \dot{\eta} \quad (10)$$

Here $J = J(\eta)$ is the inertia matrix for complete rotational kinetic energy of rotorcraft expressed in terms of generalized coordinates η . Gravitational potential energy is given by

$$U = mgz \quad (11)$$

where, z is altitude and g is acceleration due to gravity.

The Lagrangian can thus be then expressed as [7-8]

$$L = KE_{tra} + KE_{rot} - U \quad (12)$$

$$L = \frac{1}{2} (m \xi^T \dot{\xi} + \dot{\eta}^T J \dot{\eta} - 2mgz) \quad (13)$$

The model of the full rotorcraft dynamics is obtained from Euler-Lagrange equations with external generalized force F as follows:



International Journal of Advanced Research in Electrical, Electronics and Instrumentation Engineering

(An ISO 3297: 2007 Certified Organization)

Vol. 2, Issue 11, November 2013

$$\mathbf{F} = \begin{bmatrix} \mathbf{F}_\xi \\ \boldsymbol{\tau} \end{bmatrix} = \frac{d}{dt} \frac{\partial \mathbf{L}}{\partial \dot{\mathbf{q}}} - \frac{\partial \mathbf{L}}{\partial \mathbf{q}} \quad (14)$$

where $\mathbf{F}_\xi \in \mathbb{R}^3$ is the translational force applied to the rotorcraft due to main thrust i.e. control input, \mathbb{R}^3 represents generalized moments i.e. yaw, pitch and roll moments. The forces acting on rotorcraft expressed on the body frame can be written as

$$\hat{\mathbf{F}} = [0 \quad 0 \quad \mathbf{u}]^T \quad (15)$$

The translational force \mathbf{F}_ξ is related to $\hat{\mathbf{F}}$ through the equation

$$\mathbf{F}_\xi = R\hat{\mathbf{F}} \quad (16)$$

where R denotes transformation matrix representing the orientation of the rotorcraft,

$$R = \begin{bmatrix} c\theta c\psi & c\theta s\psi & -s\theta \\ s\theta c\psi s\phi - s\psi c\phi & s\theta s\psi s\phi + c\psi c\phi & c\theta s\phi \\ s\theta c\psi s\phi + s\psi c\phi & s\theta s\psi s\phi - c\psi c\phi & c\theta \end{bmatrix} \quad (17)$$

For simplicity, $c\theta$ and $s\theta$ denote $\cos\theta$ and $\sin\theta$, respectively. The generalized moments on the $\boldsymbol{\eta}$ variables are denoted by

$$\begin{aligned} \boldsymbol{\tau} &= [\tau_\phi \quad \tau_\theta \quad \tau_\psi]^T \\ \tau_\phi &= \{(\mathbf{f}_5 + \mathbf{f}_6) - (\mathbf{f}_1 + \mathbf{f}_2)\}l_1 \\ \tau_\theta &= (\mathbf{f}_3 + \mathbf{f}_4)l_2 - (\mathbf{f}_1 + \mathbf{f}_2 + \mathbf{f}_5 + \mathbf{f}_6)l_3 \\ \tau_\psi &= \sum_1^6 \tau_{M_i} \end{aligned} \quad (18)$$

where l_1 , l_2 and l_3 are the distances indicated in Fig. 1

Since the Lagrangian contains no cross terms in the kinetic energy, combining ξ and $\boldsymbol{\eta}$, the Euler–Lagrange equation can be partitioned into the dynamics for the translational ξ coordinates and the rotational $\boldsymbol{\eta}$ dynamics. So, it follows

$$\mathbf{F}_\xi = M\ddot{\xi} + m\mathbf{g} \quad (19)$$

$$\boldsymbol{\tau} = J\ddot{\boldsymbol{\eta}} + \dot{J}\dot{\boldsymbol{\eta}} - \frac{1}{2} \frac{\partial (\dot{\boldsymbol{\eta}}^T J \dot{\boldsymbol{\eta}})}{\partial \boldsymbol{\eta}} \quad (20)$$

From (16) and (19) above can be expressed as

$$M\ddot{\xi} = \mathbf{u} \begin{bmatrix} -s\theta \\ c\theta s\phi \\ c\theta c\phi \end{bmatrix} - \begin{bmatrix} 0 \\ 0 \\ m\mathbf{g} \end{bmatrix} \quad (21)$$

Defining the Coriolis terms and gyroscopic and centrifugal terms as

$$C(\boldsymbol{\eta}, \dot{\boldsymbol{\eta}})\dot{\boldsymbol{\eta}} \triangleq \dot{J}\dot{\boldsymbol{\eta}} - \frac{1}{2} \frac{\partial (\dot{\boldsymbol{\eta}}^T J \dot{\boldsymbol{\eta}})}{\partial \boldsymbol{\eta}} \quad (22)$$

$C(\boldsymbol{\eta}, \dot{\boldsymbol{\eta}})$ is the Coriolis term, which contains gyroscopic and centrifugal terms, associated with the $\boldsymbol{\eta}$ dependence of J . Finally, the dynamical model of rotorcraft is expressed as



International Journal of Advanced Research in Electrical, Electronics and Instrumentation Engineering

(An ISO 3297: 2007 Certified Organization)

Vol. 2, Issue 11, November 2013

$$M\ddot{\xi} = \mathbf{u} \begin{bmatrix} -s\theta \\ c\theta s\phi \\ c\theta c\phi \end{bmatrix} - \begin{bmatrix} 0 \\ 0 \\ mg \end{bmatrix} \quad (23)$$

$$J\ddot{\eta} = -C(\eta, \dot{\eta})\dot{\eta} + \tau \quad (24)$$

The state of the above system is given by following set of variables

$$\mathbf{X}^T \triangleq (\xi^T, \dot{\xi}^T, \eta^T, \dot{\eta}^T) = (\mathbf{x}, \mathbf{y}, \mathbf{z}, \dot{\mathbf{x}}, \dot{\mathbf{y}}, \dot{\mathbf{z}}, \theta, \phi, \psi, \dot{\theta}, \dot{\phi}, \dot{\psi}) \quad (25)$$

The state corresponding to translational displacement is defined as

$$\bar{\mathbf{x}}^T = (\mathbf{x}, \mathbf{y}, \mathbf{z}, \dot{\mathbf{x}}, \dot{\mathbf{y}}, \dot{\mathbf{z}}) \quad (26)$$

IV. CONTROL STRATEGIES

This section presents the control strategy for stabilizing the 3P-MAV6 when operating at hover. The controller synthesis monitors and regulates each state in a sequential manner using a priority rule as follows. We first stabilize the altitude of the rotorcraft using main thrust 'u'. Next we stabilize the yaw angle and then we control the roll angle ϕ and the y displacement and finally the pitch angle θ and x displacement are regulated.

TABLE I
CONTROL STRATEGY SEQUENCE

Phase	Variable	Procedure
1	Altitude, z	Main thrust; u is used to reach the desired altitude
2	Yaw, ψ	$\ddot{\tau}_\psi$ is used to set the yaw displacement to zero.
3	Roll, ϕ , y	$\ddot{\tau}_\phi$ is used to control the roll ϕ displacement along y direction.
4	Pitch, θ , x	$\ddot{\tau}_\theta$ is used to control pitch θ and the horizontal displacement along x direction.

The proposed control strategy is simple to implement and tune. The experimental setup is such that the four control inputs can independently operate in manual as well as automatic modes. For safety of flight, this feature is particularly important when implementing control strategy. The rotor craft can be operated in semi-automatic mode in which pilot control the coordinates, leaving the orientation stabilization task to control law.

Roughly, each control input can be used to regulate one or two degrees of freedom as follows: The control input u is primarily used to attain desired altitude. The control input $\ddot{\tau}_\psi$ is used to set the yaw displacement to zero. $\ddot{\tau}_\phi$ is used to control the roll angle and horizontal displacement along y direction and similarly $\ddot{\tau}_\theta$ is used to control pitch and horizontal movement along x-axis.

From equation (25), we have

$$m\ddot{\mathbf{x}} = -\mathbf{u} \sin \theta \quad (27)$$

$$m\ddot{\mathbf{y}} = -\mathbf{u} \sin \phi \cos \theta \quad (28)$$

$$m\ddot{\mathbf{z}} = -\mathbf{u} \cos \theta \cos \phi - mg \quad (29)$$

$$\ddot{\psi} = \ddot{\tau}_\psi \quad (30)$$

$$\ddot{\phi} = \ddot{\tau}_\phi \quad (31)$$



International Journal of Advanced Research in Electrical, Electronics and Instrumentation Engineering

(An ISO 3297: 2007 Certified Organization)

Vol. 2, Issue 11, November 2013

$$\ddot{\theta} = \tilde{\tau}_\theta \quad (32)$$

The control input u represents the total thrust or collective input and $\tilde{\tau}_\psi$, $\tilde{\tau}_\phi$ and $\tilde{\tau}_\theta$ represent the roll, pitch and yaw angular moments, respectively. Now, control approach is explained sequentially.

A. Altitude control

The vertical displacement along z is controlled by forcing the altitude to satisfy the dynamics of a linear system. Thus the following control input can be used

$$\mathbf{u} = (\mathbf{d}_1 + m\mathbf{g}) \frac{1}{\cos\theta \cos\phi} \quad (33)$$

where d_1 is proportional derivative (PD) controller.

$$\mathbf{d}_1 \triangleq -a_{z_1} \dot{\mathbf{z}} - a_{z_2} (\mathbf{z} - \mathbf{z}_d) \quad (34)$$

where a_{z_1} , a_{z_2} are positive constants and \mathbf{z}_d is positive constant representing desired altitude.

So, provided $\cos\theta \cos\phi \neq 0$, i.e., $\theta, \phi \in \left(-\frac{\pi}{2}, \frac{\pi}{2}\right)$ we obtain.

$$\ddot{\mathbf{z}} = \frac{1}{m} (-a_{z_1} \dot{\mathbf{z}} - a_{z_2} (\mathbf{z} - \mathbf{z}_d)) \quad (35)$$

The controller ensures $\mathbf{z} \rightarrow \mathbf{z}_d$ and $\mathbf{d}_1 \rightarrow 0$. The control parameters a_{z_1} and a_{z_2} should be carefully chosen to ensure a stable and well damped response of the rotorcraft.

B. Yaw angle control

An approach similar to altitude control is used to control yaw angle ψ also. Here also a proportional derivative (PD) controller is used. To control yaw angle, we set

$$\tilde{\tau}_\psi \triangleq -a_{\psi_1} \dot{\psi} - a_{\psi_2} (\psi - \psi_d) \quad (36)$$

$$\ddot{\psi} \triangleq -a_{\psi_1} \dot{\psi} - a_{\psi_2} (\psi - \psi_d) \quad (37)$$

where a_{ψ_1} , a_{ψ_2} are positive constants. From (36) it follows, if ψ_d is constant, then ψ converge. Therefore, $\dot{\psi}$ and $\ddot{\psi} \rightarrow 0$, which, using (37), implies $\psi \rightarrow \psi_d$.

C. Control of roll angle and horizontal displacement in y -axis.

Assuming T large enough, from equation (34) it follows that $\mathbf{d}_1 \rightarrow 0$, also from (37) $\psi \rightarrow \psi_d$, therefore (27) and (28) reduces to,

$$\ddot{x} = -g \frac{\tan\theta}{\cos\phi} \quad (38)$$

$$\ddot{y} = -g \tan\phi \quad (39)$$

The tri-copter control inputs are subject to physical constraints as in practical, maximum voltage of motors is restricted by input voltage.

So, we use the control strategy developed in [6]. The nested saturation technique developed in [6] can exponentially stabilize a chain of integrators with bounded input. The amplitudes of the saturation functions can be chosen in such a



International Journal of Advanced Research in Electrical, Electronics and Instrumentation Engineering

(An ISO 3297: 2007 Certified Organization)

Vol. 2, Issue 11, November 2013

way that, after a finite time T' the roll angle lies in the interval $-1 \text{ rad} < \theta < 1 \text{ rad}$. Therefore, for $t > T'$, $|\tan \phi - \phi| < 0.54$. Thus, after sufficient time \mathbf{d}_1 is small and the (y, ϕ) subsystem reduces to,

$$\dot{\mathbf{y}} = \mathbf{g}\phi \quad (40)$$

$$\dot{\phi} = \tilde{\tau}_\phi \quad (41)$$

This can be re-written as

$$\mathbf{y}^{iv} = \mathbf{g}\tilde{\tau}_\phi \quad (42)$$

The above equation represents four integrators in cascade.

The following control law with nested saturation is proposed:

$$\tilde{\tau}_\phi = -\mu_{\phi_1} \left(\dot{\phi} + \mu_{\phi_2} \left(\phi + \dot{\phi} + \mu_{\phi_3} \left(2\phi + \dot{\phi} + \frac{\dot{\mathbf{y}}}{\mathbf{g}} + \mu_{\phi_4} \left(\phi + 3\phi + 3\frac{\dot{\mathbf{y}}}{\mathbf{g}} + \frac{\mathbf{y}}{\mathbf{g}} \right) \right) \right) \right) \quad (43)$$

where μ_a is saturation function of the form

$$\mu_a(s) = \begin{cases} -a & s < -a \\ s & -a \leq s \leq a \\ a & s > a \end{cases} \quad (44)$$

The loop is asymptotically stable [6] and therefore $\phi, \dot{\phi}, \mathbf{y}$ and $\dot{\mathbf{y}}$ converge to zero.

D. Control of pitch angle and horizontal displacement in x-axis.

Now, it has been proved in previous section that for T large enough, $\mathbf{d}_1 \rightarrow 0$ and ϕ become sufficiently small so, that equation (27) reduces to

$$\ddot{\mathbf{x}} = -\mathbf{g} \tan \theta \quad (45)$$

$$\ddot{\theta} = \tilde{\tau}_\theta \quad (46)$$

Using a procedure similar to the one proposed for the roll control, we obtain

$$\tilde{\tau}_\theta = -\mu_{\theta_1} \left(\dot{\theta} + \mu_{\theta_2} \left(\theta + \dot{\theta} + \mu_{\theta_3} \left(2\theta + \dot{\theta} - \frac{\dot{\mathbf{x}}}{\mathbf{g}} + \mu_{\theta_4} \left(\dot{\theta} + 3\theta - 3\frac{\dot{\mathbf{x}}}{\mathbf{g}} - \frac{\mathbf{x}}{\mathbf{g}} \right) \right) \right) \right) \quad (47)$$

The above control law guarantees convergence to zero of the state $\theta, \dot{\theta}, \mathbf{x}$ and $\dot{\mathbf{x}}$.

V. SIMULATION RESULTS

The proposed non-linear control strategy has been simulated in MATLAB. The rotor-craft was initially at $(0, 0, 0, 0, 0, 0)$. The final co-ordinates assigned were $(15, 20, 30, 0, 0, 0)$. The results show that the physical angles converge to zero and the rotorcraft reaches the destination in finite time as shown in Fig. (5).

International Journal of Advanced Research in Electrical, Electronics and Instrumentation Engineering

(An ISO 3297: 2007 Certified Organization)

Vol. 2, Issue 11, November 2013

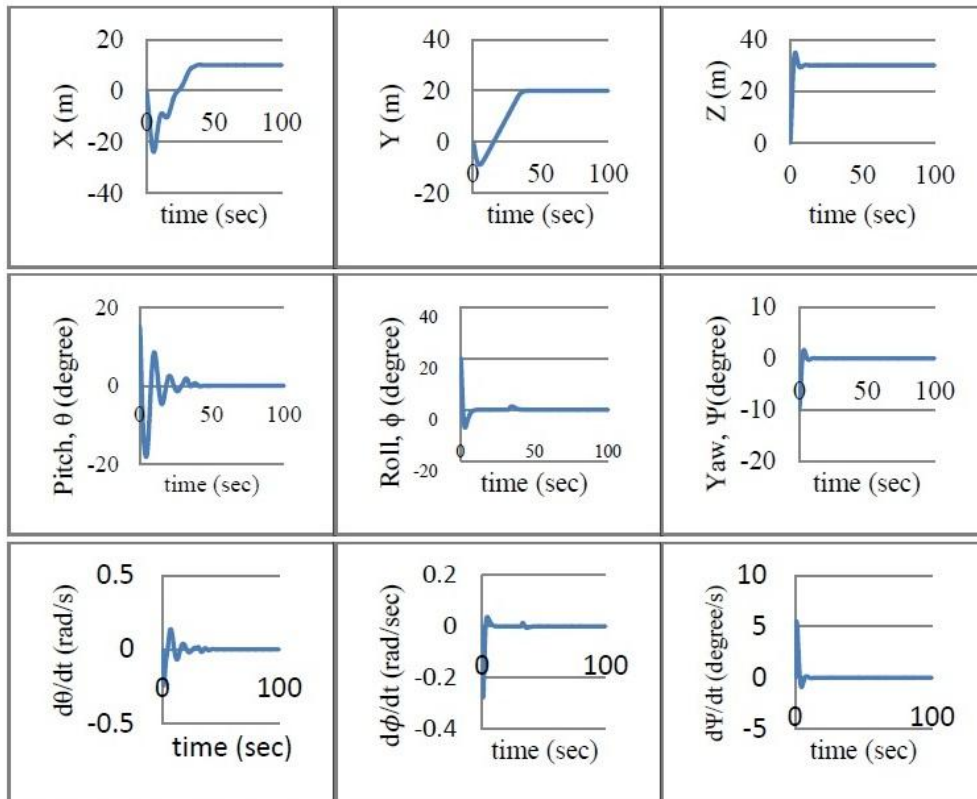


Fig. 5. Simulation Results.

VI. CONCLUSION

A novel Tri-copter, Fig. (6) which presents several advantages over the classical helicopters and quad rotors has been presented in this paper. The paper has presented a non-linear dynamical model of the tri-copter using Euler-Lagrange approach. A non-linear controller has been proposed which is based on nested saturation technique.



Fig. 6. Tricopter 3P-MAV6.



International Journal of Advanced Research in Electrical, Electronics and Instrumentation Engineering

(An ISO 3297: 2007 Certified Organization)

Vol. 2, Issue 11, November 2013

REFERENCES

- [1] Kendoul, F., Fantoni, I., and Lozano R., “Modeling and control of a small autonomous aircraft having two tilting rotors,” IEEE Transactions on Robotics, 22(6), 1297–1302, 2006.
- [2] Lozano, R., Castillo P., and Dzul, A. “Global stabilization of the PVTOL: Real time application to a mini-aircraft,” International Journal of Control, 77(8), 735-740, 2004.
- [3] Fantoni, I. and, Lozano, R. “Non-linear control for under actuated mechanical systems. In communications and control engineering series, 2002,” Book review in Automatica (Vol. 38, pp. 2030–2031). Berlin: Springer, 2002.
- [4] Kendoul, F., Alabazares, D. L., Fantoni-Coichot, I., and Lozano, R. “Real-time nonlinear embedded control for an autonomous quad-rotor helicopter,” AIAA (American Institute of Aeronautics and Astronomies) Journal of Guidance, Control, and Dynamics, 30(4), 1049–1061, 2007.
- [5] Castillo, P., Dzul, A., and Lozano, R. “Real-time stabilization and tracking of a four rotor mini rotorcraft,” IEEE Transactions on Control Systems Technology, 12, 510–516, 2004.
- [6] Teel, A. R., Global stabilization and restricted tracking for multiple integrators with bounded controls. Systems & Control Letters, 18, 165–171, 1992.
- [7] Alderete, T. S. *Simulator aero model implementation*, NASA Ames Research Center, Moffett Field, CA. Available:http://www.simlabs.arc.nasa.gov/library_docs/rt_sim_docs/Toms.pdf
- [8] McCormick, B. W., *Aerodynamics Aeronautics and Flight Mechanics*. New York: Wiley, 1995.
- [9] Olfati-Saber, R., “Global configuration stabilization for the VTOL aircraft with strong input coupling,” In Proceedings of the 39th IEEE conference on decision and control, Sydney, Australia, 2000.
- [10] Tanaka, K., Ohtake H., and Wang, H., “A practical design approach to stabilization of a 3-dof rc helicopter,” IEEE Transactions on Automatic Control, 12(2), 315–325, 2004.
- [11] Gavrillets, V., Martinos, I., Mettler, B., and Feron, E., “Control logic for automated aerobatic flight of miniature helicopter,” in Proceedings AIAA, Monterey, CA, Aug. 5–8, p. 4834, 2002.

Biography



Abhishek received the B.Tech. degree in electronics and communication engineering from Indian Institute of Technology (IIT) Guwahati, Assam, India in the year 2012. He is currently working in the field of Interval Type-2 Fuzzy Logic and his area of research is mainly focused in the field of Computation Vision, Artificial Intelligence and Robotics. He is IEEE student member and has worked previously on development of Cognitive Architecture for Robots.



Abhinandan Tripathi received the B.Tech. degree in Mechanical Engineering from Indian Institute of Technology, Guwahati, India in the year 2012. Currently he's working in Al-Khobar, Saudi Arabia as a field engineer for Schlumberger. His previous work experiences include summer internships at Rapid Manufacturing Lab in IIT Bombay, Artificial Intelligence lab, Politecnico da Milano, Italy and Bio-Engineering Lab in Tohoku University as summer research assistant. He was awarded scholarship by Honda Foundation for his work as an undergraduate engineer in 2010.